

# An integrated optical link in 140 nm SOI technology

S. Dutta<sup>1</sup>, R.J.E. Huetting<sup>1</sup>, V. Agarwal<sup>2</sup>, and A.J. Annema<sup>2</sup>

<sup>1</sup>Semiconductor Components, MESA+ Institute for Nanotechnology, <sup>2</sup>IC Design, CTIT, University of Twente, 7500AE Enschede.  
Email: [s.dutta@utwente.nl](mailto:s.dutta@utwente.nl) Phone: +31-534892312

**Abstract:** A silicon-on-insulator based optical link is introduced. Higher opto-coupling efficiency and temperature-resilience are obtained via avalanche-mode light-emitting diode operation against forward-mode operation. Self-heating induced thermo-coupling in steady-state is de-embedded by calibrating the photo-detector's photovoltaic characteristics.

**OCIS codes:** (040.6040) Silicon; (130.0250) Optoelectronics; (230.3670) Light-emitting diodes; (230.5170) Photodiodes; (130.0130) Integrated optics; (040.1880) Detection; (120.6810) Thermal effects.

## 1. Problem statement, motivation and method:

Intra-chip optical interconnects offer high speed data transfer [1] with very small form factor. The viability of such a CMOS-integrated optical link in Silicon (Si) demands a good coupling efficiency together with proper galvanic isolation. Avalanche-mode light-emitting diodes (AMLEDs) serve the first requirement as light sources [2], because of the significant overlap between their electro-luminescence (EL) spectra and the spectral responsivity of Si photo-diodes (PDs) [3], in contrast to the same system with a forward-mode (FM) LED. The second criterion can be fulfilled using Si-on-insulator (SOI) process. Prior art [4,5] report opto-coupling in a 0.35  $\mu\text{m}$  bulk process that lacks galvanic isolation, implying higher electrical crosstalk and poorer isolation voltage. However, owing to a higher electrical power dissipation ( $P$ ) and, consequently, self-heating in AMLEDs, coupling through such a link to a PD is a mix of fast optical transmission and slow thermal conduction. Therefore, it is needed to resolve these two components, which are entwined in steady-state or low-frequency operation. The LED and PD are realized with vertical n+p junctions in a 0.14  $\mu\text{m}$  SOI technology (Fig. 1(a), (d)). Galvanic isolation in the link is realized with medium trench isolation (MTI); the opto-coupling is via shallow trench isolation (STI). The opto-coupling quantum efficiency is defined as the ratio of the short-circuit current ( $I_{SC}$ ) of the PD, and the LED current ( $I$ ).  $I_{SC}$  depends on the optical intensity ( $L$ ) of the LED and absorption coefficient ( $\alpha$ ) of the PD (that increases with junction temperature,  $T_j$  [6]). The open-circuit voltage ( $V_{OC}$ ) and the  $I_{SC}$  of the PD are calibrated using an off-chip reference red LED ( $\sim 650$  nm), at well-defined ambient temperatures ( $T$ ), yielding their exclusive dependencies on  $T_j$  and  $L$ .  $V_{OC}$  can be expressed as [7],

$$V_{OC}(L, T_j) = \left(\frac{kT_j}{q}\right) \ln\left(1 + \frac{I_{SC}(L, \alpha(\lambda, T_j))}{I_0(T_j)}\right), \quad (1)$$

where  $I_0$  is the dark current, and  $\lambda$  is the photon-wavelength. Further,  $T_j = T + \Delta T = T + P \cdot R_{TH}$ , where  $R_{TH}$  is the effective thermal resistance of the system. In the AMLED,  $\Delta T$  is mainly caused by self-heating because of its relatively high  $P = P_{AM}$  ( $\sim 0.13$  W). The calibrated curves are used to estimate  $\Delta T$  in the PD by mapping the deviation in  $V_{OC}$  for AM from the calibrated curve (fitted to Eq. (1)) onto the  $V_{OC}$ - $T_j$  curve. A subsequent mapping of  $\Delta T$  onto the  $I_{SC}$ - $T_j$  curve yields the component of  $I_{SC}$  caused by the self-heating (SH)-induced rise in  $\alpha(T)$ , and is denoted here by  $\Delta I_{SC}^{(SH)}$ . Thus, the contributions of  $L$ , and  $\alpha$ , to the PD-current are decoupled. The same  $I_{SC}$  at 300 K for both (the AMLED and off-chip LED) is established for this calculation to ensure the same light absorption in the PD irrespective of the  $\lambda$ -dependency of  $\alpha$ .

## 2. Results and Conclusions

Photon emission peaks in the visible and infra-red (IR) range for the AMLED and the FMLED respectively (Fig. 1(e), (f)). The EL-micrographs are shown in Fig. 1(b) and (c), respectively. In AMLED operation,  $|I_{SC}|$  increases proportionally with  $I$  and hence with  $L$  [8]. However,  $V_{OC}$  initially increases and then decreases for higher values of  $I$  (Fig. 1(g)), signifying a thermal effect, which is negligible for the FMLED (Fig. 1(h)) since  $P_{FM} \ll P_{AM}$ . Fig. 2 outlines the aforesaid technique to extract  $\Delta T$ . Calibration with the off-chip LED shows that an increase in only  $L$  (at a fixed  $T$ ), results in an increase in both  $|I_{SC}|$  (Fig. 2(a)) and  $V_{OC}$  (Fig. 2(b)). For higher  $T$  (and fixed  $L$ ),  $V_{OC}$  decreases (Fig. 2(c)) while  $|I_{SC}|$  moderately increases, as  $\alpha$  increases (Fig. 2(d)). Owing to higher  $\alpha$  at shorter  $\lambda$ , a  $\sim 7.5$  times higher coupling efficiency and a 5 times reduction in temperature coefficient of  $I_{SC}$  are obtained in AM as compared to FM at the same  $I$  ( $= 4$  mA) for a link spacing of 28  $\mu\text{m}$  (Fig. 3(a), Table 1). Post de-embedding,  $\Delta T$  values of up to  $\sim 50$  K were extracted for AMLED operation, with a strong dependency on  $I$  (Fig. 3(b)). Fig. 3(c) shows the separated components ( $\sim 87\%$  opto-coupling,  $\sim 13\%$  thermo-coupling) of the sensed  $I_{SC}$ . To conclude, wide-spectrum opto-coupling in 0.14  $\mu\text{m}$  SOI technology is achieved for the first time. AMLED self-heating adds a thermal data path to the fast optical path, which is de-embedded using our proposed technique. The design is suitable for smart-power applications e.g. level shifters.

### References:

- [1] A. Chatterjee, B. Bhuvana, and R. Schrimpf, IEEE Elec. Dev. Lett., vol. 25, no. 9, pp. 628-630, 2004. (doi: 10.1109/LED.2004.834247)
- [2] M. du Plessis, H. Aharoni, and L.W. Snyman, "Silicon LEDs fabricated in standard VLSI technology as components for all silicon monolithic integrated optoelectronic systems," IEEE Jnl. Selected Topics in Quantum Elec., vol. 8, no. 6, pp. 1412-1419, 2002.
- [3] B.P. van Drieënhuizen, and R.F. Wolffenbuttel, "Optocoupler based on the avalanche light emission in silicon," Sensors and Actuators A, 31, pp. 229-240, 1992.
- [4] B. Huang, X. Zhang, W. Wang, Z. Dong, N. Guan, Z. Zhang, and H. Chen, Optics Communications 284 (2011) 3924-3927 (doi: 10.1016/j.optcom.2011.04.028)
- [5] A. Khanmohammadi, R. Enne, M. Hofbauer, and H. Zimmermann, Proc. 45th ESSDERC, pp. 138-141, Sept. 2015 (doi: 10.1109/ESSDERC.2015.7324732)
- [6] M.A. Green, Solar Energy Materials & Solar Cells 92 (2008), 1305-1310 (doi: 10.1016/j.solmat.2008.06.009)
- [7] B.G. Streetman, and S.K. Banerjee, "Solid state electronic devices," PHI Learning Pvt. Ltd., 6<sup>th</sup> edition.
- [8] S. Dutta, R.J.E. Huetting, A.J. Annema, L. Qi, L.K. Nanver, and J. Schmitz, "Opto-electronic modeling of light emission from avalanche-mode silicon p+n junctions," Jnl. Appl. Phys. 118 (11), 114506 (2015).

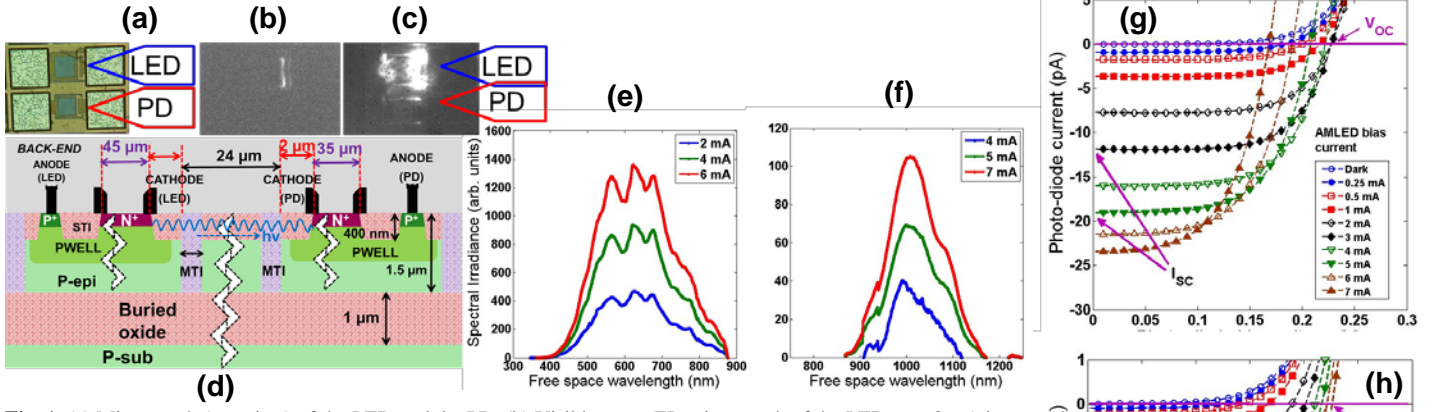


**Fig. 1:** (a) Micrograph (top-view) of the LED and the PD, (b) Visible range EL-micrograph of the LED at  $I=8$  mA in avalanche-mode (AM) captured through the XEVA-257 camera from XENICS, (c) IR-range EL-micrograph of the same LED at  $I=8$  mA in forward mode (FM) captured through the XEVA-320 InGaAs camera from XENICS. (d) Schematic cross-section of the design showing dimensions of active area and link spacing. The MTI columns ensure galvanic isolation, while the STI channel provides a low-attenuation path for photons. (e) EL-spectra (visible range) of the AMLED measured for different  $I$ . The breakdown voltage is around 16.8 V. Light is received vertically by an optical fiber feeding an ADC-1000-USB spectrometer from Avantes, (f) EL-spectra (IR-range) of the same LED in FM for different  $I$ , (g) photo-voltaic response of the PD: measured  $I$ - $V$  characteristics showing the variation in  $V_{OC}$  and  $I_{SC}$  for a varying intensity ( $L$ ) of the AMLED by adjusting  $I$ . The increase in  $|I_{SC}|$  establishes optical coupling.  $V_{OC}$  first increases and then decreases for higher  $I$  (attributed to a rise in  $T$  in PD due to self-heating in the AMLED). (h) measured  $I$ - $V$  characteristics showing the variation in  $V_{OC}$  and  $I_{SC}$  for a varying  $L$  of the FMLED by adjusting  $I$ . The heating effect is negligible for FMLED operation owing to significantly lower power dissipation.

**Table 1:** Key steady-state FOMs of the opto-coupler. Values are reported at  $T=300$  K,  $I_{LED}=4$  mA, PD dark current of  $\sim 10$  fA, and a link spacing of  $28 \mu\text{m}$ .

FOM	Coupling via AMLED	Coupling via FMLED
EL-spectrum	400-870 nm	900-1150 nm
Minimum LED supply voltage	Breakdown voltage (16.8 V)	0.7 V
Opto-coupling quantum efficiency: $\Delta I_{SC}/I_{LED}$	AMCE: $3.75 \times 10^{-9}$	FMCE: $0.5 \times 10^{-9}$
Opto-coupling power efficiency: $(\Delta I_{SC} \cdot V_{OC})/P_{LED}$	$3.60 \times 10^{-11}$	$9.46 \times 10^{-11}$
Heating in the PD: $\Delta T$	18 K	Negligible
Effective thermal resistance: $R_{TH}$	$192.47 \text{ K W}^{-1}$	---
Temperature coefficient of $I_{SC}$ : $\Delta I_{SC}/(I_{SC}(T) \cdot \Delta T)$	$0.5 \% \text{ K}^{-1}$	$2.6 \% \text{ K}^{-1}$

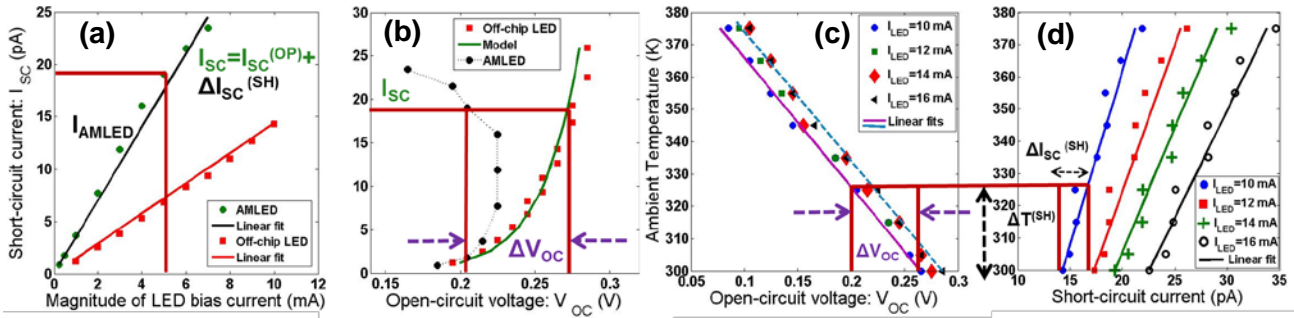


**Fig. 2:** Extraction procedure for separating contributions of  $L$  and  $\Delta T$  to  $I_{SC}$  in the PD: (a) the  $I_{SC}$  for a given input  $I$  is measured. An increase in only  $L$  (at a fixed  $T=300$  K) (red) results in an increase in  $|I_{SC}|$ . (b) The corresponding deviation in the measured avalanche-mode  $V_{OC}$  (black) from the calibrated value (using the off-chip LED at 300 K and modeled via Eq. 1 (green)) is recorded. Note that an increase in only  $L$  (red symbols) results in an increase in  $V_{OC}$ . Next, (c)  $\Delta T$  is calculated from the calibrated gradient of  $V_{OC}$ - $T$  curve of the PD. A rise in only  $T$  (for a fixed  $L$ ) leads to a decrease in  $V_{OC}$  with a mean temperature coefficient of  $-2.5 \text{ mV K}^{-1}$ . Finally, (d) the rise in  $I_{SC}$  due to the thermally induced rise in  $\alpha$  is calculated by mapping the obtained  $\Delta T$  onto the calibrated gradient of  $I_{SC}$ - $T$  curve. Note that a rise in only  $T$  (for a fixed  $L$ ) leads to a moderate increase in  $|I_{SC}|$  with a mean temperature coefficient of  $0.12 \text{ pA K}^{-1}$ .

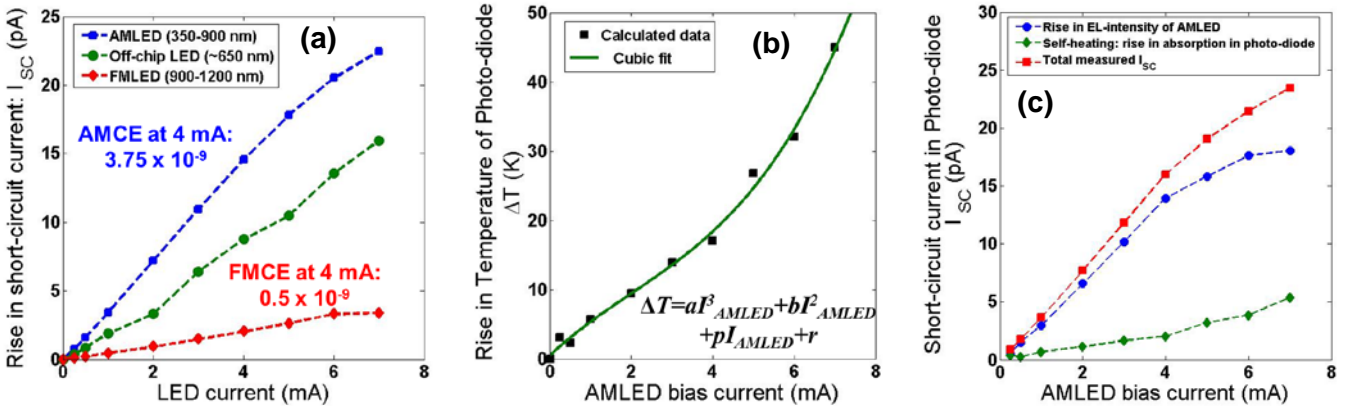


**Fig. 3:** (a) Measured  $I_{SC}$  in the PD plotted against  $I$  for the AMLED (blue), FMLED (red) and off-chip LED (green). Prior to any de-embedding, the coupling efficiency is  $\sim 7.5$  times higher for AMLED operation as compared to FMLED operation. (b) Calculated rise in temperature in the PD owing to self-heating in the AMLED, following the technique in Fig. 2. The values are fitted to the shown polynomial function where  $a=1.2 \times 10^8 \text{ A}^{-3} \text{ K}$ ,  $b=7.3 \times 10^5 \text{ A}^{-2} \text{ K}$ ,  $p=5.4 \times 10^3 \text{ A}^{-1} \text{ K}$ . The residue  $r$  (0.56 K) should be ideally zero (indicating no heating for zero current), and hence it is an indicator of goodness-of-fit of the model. (c) Resolved components of the measured  $I_{SC}$  (red) for AMLED operation against  $I$ :  $I_{SC}=I_{SC}^{(OP)}+\Delta I_{SC}^{(SH)}$ , where  $I_{SC}^{(OP)}$  (blue) is the sole contribution of  $L$  of the AMLED, while  $\Delta I_{SC}^{(SH)}$  (green) is the contribution of increased  $\alpha$  due to heating at a given AMLED bias point. 87% optical and 13% thermal coupling is obtained through the  $28 \mu\text{m}$  link.